Directing hMSCs fate through geometrical cues and mimetics peptides

Laurence Padiolleau, Christel Chanseau, Stéphanie Durrieu, Cédric Ayela, Gaétan Laroche, Marie-christine Durrieu

Directing hMSCs Fate through Geometrical Cues and Mimetics Peptides

Padiolleau L, MSc[a,b,c,d,e], Chanseau C, MSc[a,b,c], Durrieu S, BSc [f,g], Ayela C, PhD[h], Laroche G, PhD[d,e,, ‡], Durrieu M-C, PhD[a,b,c,*, ‡],*

[a]Univ. Bordeaux, Chimie et Biologie des Membranes et Nano-Objets (UMR5248 CBMN), Pessac (France)

[b]CNRS, CBMN UMR5248, Pessac (France)

[c]Bordeaux INP, CBMN UMR5248, Pessac (France)

[d]Laboratoire d'Ingénierie de Surface (LIS), Département de Génie des Mines, de la Métallurgie et des Matériaux, Centre de Recherche sur les Matériaux Avancés (CERMA), Université Laval, Québec, Canada

[e]Centre de Recherche du Centre Hospitalier Universitaire de Québec (CRCHUQ), Hôpital St-François d'Assise, Québec, Canada

[f]Université de Bordeaux, ARNA laboratory, 33076 Bordeaux, France

[g]INSERM, U1212 – CNRS UMR 5320, ARNA laboratory, 33000 Bordeaux, France

[h]Université de Bordeaux, IMS, UMR CNRS 5218, Talence F-33400, France

ABSTRACT

The native microenvironment of mesenchymal stem cells (hMSCs) – the extracellular matrix (ECM), is a complex and heterogenous environment structured at different scales. The present study aims at mimicking the hierarchical microorganization of proteins or growth factors within the ECM using the photolithography technique. Polyethylene terephthalate (PET) substrates were used as a model material to geometrically defined regions of RGD + BMP-2 or RDG + OGP mimetic peptides. These ECM-derived ligands are under research for regulation of mesenchymal stem cells osteogenic differentiation in a synergic manner. The hMSCs osteogenic differentiation was significantly affected by the spatial distribution of dually grafted peptides on surfaces, and hMSCs cells reacted differently according to the shape and size of peptide micropatterns. Our study demonstrates the presence of a strong interplay between peptide geometric cues and stem cell differentiation toward the osteoblastic lineage. These tethered surfaces provide valuable tools to investigate stem cell fate mechanisms regulated by multiple ECM cues, thereby contributing to the design of new biomaterials and improving hMSCs differentiation cues.

1. Introduction

In the field of bone tissue engineering, mesenchymal stem cells (MSCs) are considered as good potential candidates due to their high proliferation rate, multipotency and bioavailability.(1) One of the

hypotheses is that, MSCs travel from their niche to the needed site to repair the injured tissues and restore their functions.(2) The stem cell niche is a highly structured and complex microenvironment where the stem cell renewal and differentiation take place.(3) The key component of these microenvironments is the extracellular matrix (ECM). The ECM influences the MSCs fate through various stimuli, which can be biological, chemical or even mechanical. Though, the cell response depends on the abundance and distribution of the biochemical molecules in the ECM of the stem cell niche.(4) For example, during the MSCs proliferation phase, the native ECM has a higher concentration in fibroblast growth factor-2 (5) while, during the osteogenic differentiation, the ECM is richer in bone morphogenic protein-2 (BMP-2) and organization of the ECM undergoes a remodeling.(6)

Based on this knowledge, many strategies to translate the native ECM features to *in vitro* models used these growth factors to control the MSCs fate.(7,8) A traditional approach consists in the immobilization of these biochemical cues onto the surface of bioinert materials in order to mimic physiological conditions.(9) Moreover, coatings of adhesion proteins and growth factors onto materials have been used since a combination effect, regulating osteogenesis among others. It is now demonstrated that integrins plays a key role in osteogenesis while located nearby growth factors receptors.(10–13) Albeit, researchers are trying to create the ideal biomaterial through surface modification in order to satisfy the properties of the native ECM.

A promising way for the development of ideal biomaterials involves a certain level of attention to the spatial arrangement of the native ECM, which has been identified as a trigger during the stem cell differentiation.(7,14–19) As a matter of fact, during proliferation and differentiation, stem cells encounter a temporally and spatially controlled mix of biochemical cues.(20,21) This knowledge is supported by various *in vitro* studies which highlight the fact that very distinct cellular responses can be obtained through the spatial organization of ECM biomolecules.(16) Thus, biomolecules patterning of adhesion molecules and growth factors could be the next step toward the elaboration of biomaterials to mimic the native ECM *in vitro*.

By transferring the recent developments in microengineering technology to surface modification, the patterning of biomolecules onto the surface of a biomaterial can now be performed. The field of biomaterials has been extensively using microfabrication techniques to replicate the complexity of the native ECM.(22) The study presented herein describes a technique to spatially pattern two mimetic peptides onto a model material, polyethylene terephthalate (PET) films. The peptides used in this study are RGD, a cell adhesion promoter, and BMP-2 or OGP_{10-14} (osteogenic growth peptide), to induce stem cell osteogenic differentiation.(13,23,24) The RGD sequence and BMP-2 mimetic peptides are known to act synergistically to promote osteogenic differentiation when randomly co-tethered onto a biomaterial surface.(18,23,25) Spatial organization of ECM biomolecules has already been used to control MSCs fate, but with confined single cells

(26,27) or with different cell type.(28,29) Moreover, most of these studies were focusing on the impact of organized tethered ligands on cellular adhesion. Our approach combined a cell adhesion promoter – the RGD peptide – and peptides known to induce osteogenic differentiation – the BMP-2 mimetic peptide and OGP_{10-14}. These peptides were combined according to different shapes (squares, rectangles, hexagons) or different square sizes at the micrometric scale to control the cell adhesion while promoting the osteogenic differentiation, to closely mimic the native ECM and gather information about the stem cell interaction with their microenvironment.

2. Materials and Methods

2.1. Materials

PET samples were taken from a commercial crystalline biaxially-oriented film obtained from GOODFELLOW (LILLE, France). The bi-oriented film had a thickness of 75 µm. Inorganic reagents (NaOH, $KMnO_4$, H_2SO_4, HCl, glacial acetic acid), acetone, acetonitrile, dimethylaminopropyl-3-ethylcarbodiimideethylcarbodiimide hydrochloride (EDC), N-hydroxysuccinimide (NHS) and 2-(N-morpholino)-ethanesulfonic acid (MES), and toluidine blue-O (TBO) were purchased from SIGMA-ALDRICH (LYON, France). GRGDSPC (RGD), GYGFGG (OGP), RKIPKASSVPTELSAISMLYL, which is a BMP-2 mimetic peptide previously identified by our group (BMP-2) (18,19,30), GRGDSPC-TAMRA, and RKIPKASSVPTELSAISMLYL-FITC fluorescent peptides were synthesized by GENECUST, (ELLANGE, Luxembourg).

2.2. Methods

2.2.1. Surface preparation of PET and covalent grafting of the different peptides

PET surfaces were modified according to Chollet *et al.* (31) with some modifications. Briefly, PET was hydrolyzed and oxidized in order to create carboxyl groups on the surface (labeled as ''PET-COOH''). Then, the surfaces were immersed in a solution of EDC (0.2 M) + NHS (0.1 M) + MES (0.1 M) in MilliQ water for activation.

2.2.2. Preparation of resist patterned surfaces

Resist patterns were created on glass substrates using photolithography. Briefly, photosensitive resist S1818 (CHIMIE TECH, France) was coated on glass surfaces and spun at 3000 rpm for 30 s, leading to a homogenous photoresist of approximately 1 µm. The surfaces were then baked at 100 °C for 60 s prior exposure to a pattern of light emitted by UV lamp (365 nm, 19,5 mW/cm², contact mode, 50 Hz, exposure time: 8 s) through photomasks with patterns of different geometries (see Figure 1) (Département de génie électrique et de génie informatique, Université de Sherbrooke, QC, Canada). Subsequently, the exposed resist was developed by immersing the substrates in Microposit Developer solution (MF319, CHIMIE TECH, France) for 40 s. Finally, the samples were washed with deionized water, to remove any traces of developed resist, and dried with nitrogen gas (Figure 1).

2.2.3. Peptide grafting and patterning

The covalent grafting of peptides was achieved as described in a previous publication.(32) Briefly, the activation step was followed by creating resist patterns on activated surfaces using photolithography

as described in the previous paragraph. Finally, resist patterned surfaces were immersed in peptide solution (peptides dissolved in PBS at the concentration of 10^{-5}M) for 16h at room temperature. After reaction, samples were washed with deionized water under agitation, and then immersed in acetone for 30 seconds to remove the resist pattern, resulting in peptide patterns surrounded with activated domains. Then the second peptide was grafted following the same protocol. Finally, substrates were rinsed and sonicated with MilliQ water (Figure 2). Patterns of RGD-TAMRA and BMP-2-FITC or OGP-FITC peptides developed using this protocol were shaped as hexagons, squares or rectangles (Figure 1). Unpatterned and unfunctionalized PET surfaces functionalized were also prepared and used as controls for biological experiments.

2.2.4. Surface characterization

The covalent grafting of peptides, the density of grafted peptides as well as the surface roughness after each step of surface modification were evaluated in a previous work on unpatterned PET surfaces using X-ray photoelectron spectroscopy, fluorescence microscopy, contact angle, and atomic force microscopy (32). In the present work, we have focused on evaluating the efficiency of peptide patterning using fluorescence microscopy and optical interferometry. On resist patterned surfaces, fluorescence microscopy (LEICA DM5500B, WETZLAR, Germany) was used to characterize the shape of resist patterns while optical interferometry (Bruker Nano-NT9080, KARLSRUHE, Germany) was employed to measure the pattern dimensions. Resist patterns were

visible under fluorescence because the S1818 resist is auto-fluorescent when excited with a 543nm laser line. Optical interferometry measurements were carried out on dry samples, at room temperature, using the vertical scanning interferometry mode with a vertical resolution of approximately 2 nm. The interferograms were digitalized with a CCD camera and converted into 2D topographic maps. Pattern dimensions, according to the X and Y axes, were measured on these maps using Veeco software.

These PET surfaces containing resist patterns were then used as a template for fluorescent RGD and BMP-2 or OGP patterning. Finally, the spatial distribution of peptides was visualized under fluorescence microscopy (Leica microsystem DM5500B, microscope with a motorized, programmable stage using a CoolSnap HQ camera controlled by Metamorph 7.6).

2.2.5. Cell culture

Human mesenchymal stem cells (hMSCs) from bone marrow (one donor) purchased from PromoCell (Heidelberg, Germany), were grown in mesenchymal stem cell basal media (MSCBM2) (PromoCell) in a humidified atmosphere containing 5% (vol/vol) CO_2 at 37 °C. For each experiment, hMSCs between passages 4 and 5 were seeded on PET materials at at an identical density of 5,000 cells/cm² for all materials in serum-free α-MEM during the first 6 h. The medium was then changed to α-MEM supplemented with 10% (v/v) fetal bovine serum FBS (Gibco) with no additional growth factors and was changed every 72 h. hMSC

differentiation on the different PET substrates was evaluated after 2 weeks of cell culture. Due to the large number of materials (more than 140 materials) required to perform the biological analyses, the decision was made to perform cell cultures at one specific time point.

2.2.6. RT Quantitative Real-Time PCR

hMSCs were lyzed in TRIZOL reagent (Invitrogen) to isolate the total RNA. TurboDNA free kit (Ambion) was used to remove contaminating DNA from RNA preparations. 2 µg of purified total RNA were used to synthesize cDNA using Thermo Scientific Maxima Reverse Transcriptase (Thermo Scientific) and random primers (Thermo Scientific). cDNA aliquots (4 ng) were then amplified in 10 µL reaction volume containing 500 nM primers and SsoAdvancedTM Universal SYBR® Green Supermix (Biorad) using CFX96TM Real-Time PCR Detection System (Biorad). PCR cycling parameters were as follow: denaturation at 95 °C for 30 s followed by 40 cycles of PCR reactions (95 °C for 5 s and 60 °C for 10 sec). Cq values for the gene of interest were normalized against two genes: RPC53 and PPIA. Bestkeepper software was used to determine normalization effectiveness of each reference gene among all samples. The relative expression levels were calculated using the comparative method (2-ΔΔCt) and controls were arbitrarily set at 1. Primers used for amplification are listed in Table 1.

2.2.7 Statistical Analyses

All data were expressed as the mean ± standard deviation (SD) and analyzed by one-way analysis of variance (ANOVA) and Tukey's test for multiple comparisons, using GraphPad Prism version 6.01 for Windows

(GraphPad Software, San Diego, CA, USA, www.graphpad.com). Significant differences were determined for p values of at least ≤ 0.05. * p ≤ 0.05, ** p ≤ 0.01, and *** p ≤ 0.001.

3. Results

3.1. Characterization of patterned surfaces

The grafting protocol to conjugate peptides on the patterned surfaces was previously described.(18) Photolithography was used on activated surface (PET-NHS) to create resist patterns. All the surfaces with the resist patterns were assessed under fluorescence microscopy due to the S1818 resist auto-fluorescence. Images clearly showed the precise geometries shaped as hexagons, rectangles and squares (Figure 3). After the qualitative assessment of the resist patterned surfaces, the quantitative assessment of these surfaces was performed using optical interferometry. The obtained surface profiles revealed that resist pattern sizes are closed to the originally defined micro-sized features (Table 2 and Figure 3).

Then, the first fluorescent peptide to be grafted (RGD-TAMRA) was putted into contact with the resist micropatterned surfaces. Therefore, only the available area was grafted with the first peptide. After removing the resist, the surfaces were placed into a solution of the second peptide to graft (BMP-2-FITC or OGP-FITC). Fluorescence microscopy confirmed the efficiency of peptide patterning. Images showed identifiable patterns and exhibit the expected shapes (hexagonal, squared and rectangular geometries) and size (Figure 4),

and the intensity profile exhibits no overlap of the different regions (Figure 5). Surfaces for cell culture were produce in the exact same way, from the same batch of materials.

3.2. hMSCs osteogenic differentiation

First, it is worth mentioning that a previous work investigated the effect of the homogeneous conjugation of individual peptides (RGD, BMP-2, and OGP) (32). With few exceptions, these single-tethered peptide surfaces exhibited lower expressions for all three markers (RUNX2, collagen I α-1, and OCN) investigated in the present study, therefore pointing to a synergistic effect toward cell differentiation when the so-called adhesion and differentiation signal peptides were co-conjugated on a surface. Accordingly, any additional marker expression response measured while comparing homogeneous surface conjugation of the adhesion peptide (RGD) together with a differentiation peptide (BMP-2 or OGP) can only be attributed to pattern shapes or sizes.

3.2.1. The extent of hMSCs osteogenic differentiation in response to different shapes of patterns

The potential changes in hMSCs phenotype on the different shapes of patterned surfaces were assessed by RT-qPCR after 2 weeks of cell culture. Human MSCs seeded on oxidized PET in the same cell culture conditions were used as negative control. Surfaces conjugated with a mixture of RGD and BMP-2 peptides were first investigated. At first sight, the results showed that the expression of RUNX2, an early osteogenic marker, was significantly enhanced in the cells cultured on the tethered surfaces, as compared to control surfaces (Figure 6A). On

the other and, the organization of RGD and BMP-2 peptides as squares, hexagons, or rectangles did not lead to additional RUNX2 expression as compared to the surface randomly conjugated with the mixture of peptides. Similar trends were observed while considering ColI-α1 expression, with significant differences recorded when RGD and BMP-2 are patterned as rectangles and hexagons as compared to the control sample or to the surface homogeneously coated with both peptides (Figure 6B). Finally, the OCN expression did not allowed to discriminate among all investigated samples, likely because that the culture time that was investigated in the present study was not long enough to allow measuring differences in this marker expression (Figure 6 C).

Surfaces with a mixture of RGD and OGP were also investigated. In this case, the situation is less clear in terms of RUNX2 expression. Indeed, the presence of both RGD and OGP on the various investigated samples clearly lead to an increase of the RUNX2 expression as compared to the control sample (Figure 6D). However, no significant differences were evidenced among the various investigated patterns. That said, the expression of ColI-α1 shed more light on the effect of the RGD and OGP organization on the surfaces as the squares definitely lead to a significant increase of this marker with respect to all other investigated samples (Figure 6E).
Again, it sounds that the culture time was not long enough to enable measuring differences in the OCN expression, therefore

providing an indication about the state of the differentiation level (Figure 6F).

Taken together, the data on both the RGD/BMP-2 and RGD/OGP surface patterning point toward an improved cell differentiation related to the peptide couple organization on the surface. In addition, it is also clear that an identical geometrical organization of the RDG/BMP-2 and RGD/OGP couples was not felt similarly by the HMSCs in terms of their differentiation.l.

3.2.2. The extent of hMSCs osteogenic differentiation in response to different size of patterns

The potential changes in hMSCs phenotype on the surfaces patterned with different sizes of squares were assessed by RT-qPCR after 2 weeks of cell culture (Figure 7). Human MSCs seeded on oxidized PET in the same cell culture conditions were used as negative control. Surfaces with a mixture of RGD and BMP-2 peptides were first investigated. With the

exception of the 100x100 sample, the expression of RUNX2 (Figure 7A) is more important on the RGD/BMP-2 tethered surfaces (random, 50x50 and 25x25) as compared with the control sample, with the most important expression being observed on the smallest size of square pattern. Of note, a nice gradation of the RUNX2 expression was observed from the larger (100x100) to the smaller (25x25) RGD/BMP-2 tethered surfaces. For the RGD/BMP-2 couple, the importance of the pattern size on the cell differentiation behavior was also observed while measuring the collagen I α-1 and OCN expression (Figure 7B and 7C), as both markers exhibited the highest measured level among all investigated samples when cells were cultured on the 25x25 pattern.

The situation was somewhat different while investigating the effect of peptide pattern size with the RGD/OGP couple. On one hand, the random, 100x100, and 50x50 samples all led to an almost equivalent four-fold increase of the RUNX2 expression (Figure 7D) as compared to the control sample. On the other hand, the expression of RUNX2 was again higher on the smaller size pattern, that is the 25x25 sample. In this case, this marker level of expression was eight times that of the control sample and twice that of any other investigated RGD/OGP conjugated surfaces, either homogeneously conjugated or patterned. For this peptide couple, the expression of ColI-α1 (Figure 7E) was significantly higher only in the case of the medium size (50x50) and OCN (Figure 7F) was not significantly impacted by the tethered peptides in any cases.

~~3~~4. Discussion

Promoting a specific fate of hMSCs is a complex process involving different parameters such as cell morphology, gene expression and ECM protein concentration changes. *In vivo*, the osteogenic differentiation process is ruled through different stimuli, which can be chemical and/or physical in nature.(3,4) The differentiation of hMSCs in the stem cell niche is guided by those stimuli. *In vitro*, scientists are trying to reproduce the stem cell niche to promote stemness or induce a guided differentiation. The use of peptide appears to be a good solution to mimic the stem cell niche. For example, BMP-2 mimetic peptides were used *in vitro*,(18,23,33) in animal models (34) and are FDA approved for various surgeries such as spinal cord fusion procedure.(35,36) However, to overcome the diffusion of the mimetic peptide away from the implant when placed in the body, immobilization on biologically compatible biomaterials surface can be used.(37)

Osteogenesis is induced thought the interaction of BMP-2 growth factor with its receptor – BMP transmembrane receptors type I and type II (BMPR-I and BMPR-II). BMP-2 preferentially interact with BMPR-II which activate the phosphorylation of SMAD1/5/8 and their translocation into the nucleus. Following the translocation, RUNX2 expression is significantly improved as another early markers regulating osteoblast differentiation.(38) The expression of RUNX2 further activates the upregulation of osteoblast phenotypes proteins.(39) Although BMP-2 peptide is greatly used in biomaterial strategies to promote bone regeneration, current strategies for the design of biomaterials for

bone tissue engineering are using multiple peptides combined on the surface of a biomaterial.(18,19,23) This strategy is used to mimic the physiological situation, where a combinatorial effect of a mixture of ligands synergize together to induce the differentiation process. Ligand crosstalk has been investigated in order to differentiate stem cells. For example, various combinations of BMP-2 (sequence used KIPKASSVPTELSAISTLYL), osteopontine (OPN) and RGD were used to induce the differentiation of rate MSCs cells.(40) An increase of ALP activity and calcium content after 2 and 4 weeks on the hydrogels containing RGD alone, and even further with the hydrogels containing the mixture of RGD and BMP-2 and/or OPN. We recently demonstrated that the expression of alkaline phosphatase is more important on surfaces tethered with FHRRIKA and BMP-2 peptides together, without requiring differentiation media during the cell culture.(32)

Another growth factor which can induce hMSCs differentiation is osteogenic growth peptide (OGP). This peptide has demonstrated an ability to upregulate~~d~~ the differentiation of hMSCs and to promote the mineralization of the matrix. Different studies demonstrated that its capabilities are dependent to its concentration however it is independent to the fact that the peptide is present in a soluble form of tethered on the surface of a material..(13,24,41) The OGP sequence has also been used in combination with the RGD sequence in order to differentiate pre-osteoblasts (MC3T3) into osteoblasts on polymer substrates (polyethylene oxide).(13) It is believed that the RGD sequence binds to the integrins while the OGP sequence (no receptor

identify up to date) causes differentiation into bone cells.(42) The combination of these two peptides might enables cells to adhere and differentiate on the same surface. Furthermore, we recently demonstrated that the expression of OPN and RUNX2 is increased in cells cultivated on PET surfaces tethered with RGD and OGP after two weeks, without the addition of differentiation media.(32)

The level of organization of the ECM ranges from the nano- to the micro-scale. The present work aimed to mimic the micro-organization. Pattern shapes (squares, rectangles, hexagons) have been inspired from previous studies that reported that elongated and angular shapes preferentially promote the differentiation toward osteoblastic cells.(14,43,44) We have investigated similar sizes of the different shapes of patterns with a combination of RGD and a growth factor mimicking peptide (either BMP-2 or OGP) compared to a random distribution. However, it is now demonstrated that biochemical cues distribution is not homogeneous within the ECM (45) and cells might be sensitive to different size of pattern on a surface. Therefore, different sizes of the square patterns were also investigated.

As shown in the results sections, hMSCs sense and respond to the various size of dual peptide micropatterns. Indeed, the smallest size of squares (25x25 μm^2) significantly enhanced RUNX2 expression after two weeks of cell culture, whereas the largest sizes of patterns have a similar response compared to randomly grafted peptide samples. These results deliver indications that the hMSCs differentiation process can

be triggered through both biochemical and geometric cues. Therefore, the micro organization of the peptides as specific patterns appears to be critical during the hMSCs differentiation.

The use of micro-sized geometric patterns to control the stemness character or induce stem cell differentiation is a rather recent topic. Accordingly, few studies demonstrated the link between microscale distribution and MSCs differentiation into specialized phenotypes. McBeath *et al.* have used fibronectin islands onto polydimethylsiloxane of different sizes (1024, 2025, and 10 000 μm²) to culture MSCs for 1 week in mixed osteogenic/adipogenic media.(43) The results of this study show that MSCs cultured on the largest micro-islands mainly differentiate into osteoblasts, whereas those on smaller micro-islands exhibits adipocytes characteristics. In our study, the most advanced differentiation process is on the smallest pattern (625 μm²) as compared to the largest pattern (10 000 μm²) and the random grafting. That said, McBeath *et al.* made their investigation on a single pattern element studying a single cell while the present study rather focused on arrays of biofunctionalized patterns. Therefore, the cell environment and the material on which the cells are cultured are different and can lead to different results. The material can have a great impact depending on the material hydrophilicity, charge, mechanical properties.

Another study investigated the fate of MSCs on RGD patterns of different geometries (circles, squares, triangles and stars) of 900

µm² on a poly(ethylene glycol) hydrogel.(14) In this study, the optimal osteogenesis was observed on the star shape after one week of culture. Whereas scientists still does not fully understand why specific geometrical cues are able to induce the differentiation toward the osteoblastic lineage, some tried to defined a general signaling pathway.(14,15,43) In the current study, the use of different shapes of grafted peptides appears to impact on the differentiation of stem cells compared to the randomly tethered surfaces. As the expression of ColI-α1 was significantly higher in the case of the cells cultured on rectangle-patterned surfaces with both RGD and BMP-2, this means these cells are committed to the osteoblastic lineage.(46) In addition, the cells in contact with the RGD/OGP peptide couple exhibit a stronger engagement while cultured on surfaces presenting hexagonal and rectangular features. In a previous study of our group,(32) the possible synergetic effect between RGD and OGP was investigated and it was demonstrated that the OGP sequence is more efficient to promote an osteoblastic differentiation in presence of the RGD sequence while grafted randomly on the surface of PET. In the present study, we demonstrate that this synergetic effect between RGD and OGP peptide is further enhanced while the peptides are tethered following a specific shape (hexagonal or rectangular).

Although our study provides clear evidence that hMSCs can sense geometrical cues in their environment, it appears that the size of these patterns is also an important factor to consider the differentiation process. Bilem *et al.* showed that the geometrical

peptide arrangement was important to guide hMSCs differentiation using smaller pattern than the ones used in the present study.(18) However, the size of the investigated patterns in Bilem et al. work was between 10 to 200 times smaller than the patterns investigated in the present study. With the present data, cells cultured on the smallest patterns – independently from the peptide couple investigated – exhibit strong RUNX~~unx-~~2 expression and a higher expression of ColI-α1 and OCN in the case of RGD/BMP-2 peptide couple. Therefore, the pattern size appears as the most important factor to consider when designing peptide patterns on a flat surface for hMSCs differentiation. However, since the random grafting of peptide, which can be considered as the smallest size of pattern we can create, did not induce further differentiation of the cells into the osteoblastic lineage, it can be hypothesized that cells are responsive to geometrical features until a minimum feature size. In addition, among the three investigated markers, RUNX2 was clearly the first to be expressed. As RUNX-2 is the first of the three markers to be expressed during osteogenic differentiation, (46), it is likely that the differentiation of the cells cultured on the patterned surfaces with basal media is at an early stage, but nevertheless engaged into the process. Of note, some of the data presented herein sometimes showed differentiation through the ColI-α1 gene expression, without clear signs of differentiation coming from the RUNX2 marker. However, these results were repeatedly measured. As of now, the reason for such a behavior remains unclear.

By combining the results of the present investigation and literature, we can draft the composite picture of an ideal biomaterial to induce a fast differentiation toward the osteoblast lineage. Indeed, according to our data, hMSCs differentiation into osteoblasts is promoted by using a combination of RGD and BMP-2 peptide arranged on a flat surface,(18,23) tethered on the surface using sharp motifs,(47) preferentially elongated such as rectangles, and using a pattern size equal or smaller than 625 μm^2.

This ideal material would be the best one to differentiate hMSCs toward the osteoblastic lineage as our results show a higher expression of RUNX2 (4 times higher) and an expression of OCN that is twice higher (compared to the control) within 2 weeks of cell culture without using osteogenic media.

Further investigations are required to fully understand these observations. However, it is likely that the smallest patterns lead to much more crosstalk between RGD and BMP-2 or OGP, therefore regulating the signalization pathways. Indeed, it is well established that RGD peptides affect the colocalization of integrin and ligand receptors which in turn, leads to cell commitment and differentiation.(17)

~~4~~5. Conclusion

2D model materials were engineered to investigate the impact of the geometry and size micro-scale distribution of RGD peptides combined with an osteogenic inducer peptide (BMP-2 or OGP). We have recently

demonstrated that homogeneously co-conjugated RGD/BMP-2 or RGD/OGP peptides onto PET surfaces significantly enhanced hMSCs osteogenesis as compared to the solely homogeneous grafting of BMP-2 or OGP peptides. In the present study, we demonstrated that these same combinations of peptides can further induce stem cell differentiation when appropriately organized on the surface. The patterning must be relatively small (area less than 625 μm^2) and sharp in terms of their shapes (such as rectangles). Among all the concentrations that were assessed, a 50/50 combination of RGD and BMP-2 appears to be the best mixture to promote osteogenic differentiation. Taken together, these results suggest that the combination of chemical and geometric cues is able to direct stem cell fate without the need of differentiation media. This surface modification strategy provides a versatile platform for surface structuration and its optimization for various biomaterials applications.

AUTHOR INFORMATION

Corresponding Author

* gaetan.laroche@gmn.ulaval.ca

* marie-christine.durrieu@inserm.fr

Author Contributions

The manuscript was written through contributions of all authors. All authors have given approval to the final version of the manuscript.

‡These authors contributed equally.

Funding Sources

The authors thanks Laurent Plawinski for the constructive discussions over RT-qPCR results. L. Padiolleau acknowledges funding from the IDEX Bordeaux and NSERC – Canada CREATE Program of Regenerative Medicine (NCPRM). The authors would like to thank the French Agence Nationale de la Recherche (ANR-13-BS09-0021-02) (M.C.D). This research was supported by the National Research and Engineering Research Council of Canada (G.L.).

ABBREVIATIONS

MSCs, mesenchymal stem cells; ECM, extracellular matrix; BMP-2: bone morphogenic protein-2; PET: polyethylene terephthalate; EDC: dimethylaminopropyl-3-ethylcarbodiimideethylcarbodiimide hydrochloride; NHS: N-hydroxysuccinimide; TBO: toluidine blue-O: hMSCs: human mesenchymal stem cells; OCN: osteocalcin; ColI-α1: collagen I α1

REFERENCES

1. Ullah I, Baregundi Subbarao R, Rho G-J. Human Mesenchymal Stem Cells - Current trends and future prospective. Biosci Rep [Internet]. Portland Press Ltd; 2015 Apr 28 [cited 2017 Oct 9];35(2):e00191. Available from: http://www.ncbi.nlm.nih.gov/pubmed/25797907

2. Fong ELS, Chan CK, Goodman SB. Stem cell homing in musculoskeletal injury. Biomaterials. 2011;32(2):395–409.

3. Jones DL, Wagers AJ. No place like home: anatomy and function of the stem cell niche. Nat Rev Mol Cell Biol. 2008;9(1):11–21.

4. Keung AJ, Kumar S, Schaffer D V. Presentation Counts: Microenvironmental Regulation of Stem Cells by Biophysical and Material Cues. Annu Rev Cell Dev Biol. 2010;26(1):533–56.

5. Tsutsumi S, Shimazu A, Miyazaki K, Pan H, Koike C, Yoshida E, et al. Retention of Multilineage Differentiation Potential of Mesenchymal Cells during Proliferation in Response to FGF. Biochem Biophys Res Commun. 2001;288(2):413–9.

6. James AW. Review of Signaling Pathways Governing MSC Osteogenic and Adipogenic Differentiation. Scientifica (Cairo). 2013;2013:1–17.

7. Akhmanova M, Osidak E, Domogatsky S, Rodin S, Domogatskaya A. Physical, Spatial, and Molecular Aspects of Extracellular Matrix of in Vivo Niches and Artificial Scaffolds Relevant to Stem Cells Research. Stem Cells Int. 2015;2015.

8. Lutolf MP, Blau HM. Artificial stem cell niches. Adv Mater. 2009;21(32–33):3255–68.

9. Hubbell JA. Bioactive biomaterials. Vol. 10, Current Opinion in Biotechnology. 1999. p. 123–9.

10. Park JS, Yang HN, Jeon SY, Woo DG, Na K, Park KH. Osteogenic differentiation of human mesenchymal stem cells using RGD-modified BMP-2 coated microspheres. Biomaterials. 2010;31(24):6239–48.

11. Fourel L, Valat A, Faurobert E, Guillot R, Bourrin-Reynard I, Ren K, et al. β3 integrin-mediated spreading induced by matrix-bound

BMP-2 controls Smad signaling in a stiffness-independent manner. J Cell Biol. 2016;212(6):693–706.

12. Rasi Ghaemi S, Delalat B, Cetó X, Harding FJ, Tuke J, Voelcker NH. Synergistic influence of collagen i and BMP 2 drives osteogenic differentiation of mesenchymal stem cells: A cell microarray analysis. Acta Biomater. 2016;34:41–52.

13. Moore NM, Lin NJ, Gallant ND, Becker ML. The use of immobilized osteogenic growth peptide on gradient substrates synthesized via click chemistry to enhance MC3T3-E1 osteoblast proliferation. Biomaterials [Internet]. Elsevier Ltd; 2010;31(7):1604–11. Available from: http://linkinghub.elsevier.com/retrieve/pii/S014296120901223X

14. Peng R, Yao X, Ding J. Effect of cell anisotropy on differentiation of stem cells on micropatterned surfaces through the controlled single cell adhesion. Biomaterials. 2011;32(32):8048–57.

15. Yao X, Peng R, Ding J. Effects of aspect ratios of stem cells on lineage commitments with and without induction media. Biomaterials. 2013;34(4):930–9.

16. Lim JY, Donahue HJ. Cell Sensing and Response to Micro- and Nanostructured Surfaces Produced by Chemical and Topographic Patterning. Tissue Eng [Internet]. 2007;13(8):1879–91. Available from: http://www.liebertonline.com/doi/abs/10.1089/ten.2006.0154

17. Ekerdt BL, Segalman RA, Schaffer D V. Spatial organization of cell-adhesive ligands for advanced cell culture. Vol. 8, Biotechnology Journal. 2013. p. 1411–23.

18. Bilem I, Plawinski L, Chevallier P, Ayela C, Sone ED, Laroche G, et al. The spatial patterning of RGD and BMP-2 mimetic peptides at the subcellular scale modulates human mesenchymal stem cells osteogenesis. J Biomed Mater Res Part A [Internet]. 2017 Dec 1 [cited 2018 Jan 3];(418). Available from: http://doi.wiley.com/10.1002/jbm.a.36296

19. Bilem I, Chevallier P, Plawinski L, Sone ED, Durrieu MC, Laroche G. RGD and BMP-2 mimetic peptide crosstalk enhances osteogenic commitment of human bone marrow stem cells. Acta Biomater. 2016;36:132–42.

20. Ramel MC, Hill CS. Spatial regulation of BMP activity. Vol. 586, FEBS Letters. 2012. p. 1929–41.

21. Lutolf MP, Gilbert PM, Blau HM. Designing materials to direct stem-cell fate. Nature [Internet]. 2009;462(7272):433–41. Available from: http://www.nature.com/doifinder/10.1038/nature08602

22. Thery M. Micropatterning as a tool to decipher cell morphogenesis and functions. J Cell Sci [Internet]. 2010;123(24):4201–13. Available from: http://jcs.biologists.org/cgi/doi/10.1242/jcs.075150

23. Zouani OF, Chollet C, Guillotin B, Durrieu M-C. Differentiation of pre-osteoblast cells on poly(ethylene terephthalate) grafted with RGD and/or BMPs mimetic peptides. Biomaterials [Internet]. Elsevier Ltd; 2010;31(32):8245–53. Available from: http://linkinghub.elsevier.com/retrieve/pii/S0142961210008859

24. Panseri S, Russo L, Montesi M, Taraballi F, Cunha C, Marcacci M, et al. Bioactivity of surface tethered Osteogenic Growth Peptide motifs. Medchemcomm [Internet]. 2014;5(7):899. Available from: http://xlink.rsc.org/?DOI=c4md00112e

25. Zouani OF, Rami L, Lei Y, Durrieu M-C. Insights into the osteoblast precursor differentiation towards mature osteoblasts induced by continuous BMP-2 signaling. Biol Open [Internet]. 2013;2(9):872–81. Available from: http://www.pubmedcentral.nih.gov/articlerender.fcgi?artid=3773333&tool=pmcentrez&rendertype=abstract

26. McBeath R, Pirone DM, Nelson CM, Bhadriraju K, Chen CS. Cell shape, cytoskeletal tension, and RhoA regulate stem cell lineage commitment. Dev Cell. 2004;6(4):483–95.

27. Kilian KA, Bugarija B, Lahn BT, Mrksich M. Geometric cues for directing the differentiation of mesenchymal stem cells. Proc Natl Acad Sci U S A [Internet]. 2010 [cited 2017 Feb 24];107(11):4872–7. Available from: http://www.pubmedcentral.nih.gov/articlerender.fcgi?artid=2841932&tool=pmcentrez&rendertype=abstract

28. Lagunas A, Comelles J, Oberhansl S, Hortigüela V, Martínez E, Samitier J. Continuous bone morphogenetic protein-2 gradients for concentration effect studies on C2C12 osteogenic fate. Nanomedicine Nanotechnology, Biol Med. 2013;9(5):694–701.

29. Oberhansl S, Castano AG, Lagunas A, Prats-Alfonso E, Hirtz M, Albericio F, et al. Mesopattern of immobilised bone morphogenetic

protein-2 created by microcontact printing and dip-pen nanolithography influence C2C12 cell fate. RSC Adv. 2014;4(100):56809–15.

30. Zouani OF, Kalisky J, Ibarboure E, Durrieu M-C. Effect of BMP-2 from matrices of different stiffnesses for the modulation of stem cell fate. Biomaterials [Internet]. Elsevier Ltd; 2013;34(9):2157–66. Available from: http://dx.doi.org/10.1016/j.biomaterials.2012.12.007

31. Chollet C, Chanseau C, Rémy M, Guignandon A, Bareille R, Labrugère C, et al. The effect of RGD density on osteoblast and endothelial cell behavior on RGD-grafted polyethylene terephthalate surfaces. Biomaterials. 2009;30:711–20.

32. Padiolleau L, Chanseau C, Durrieu S, Plawinski L, Chevallier P, Laroche G, et al. Study of single or mixture of tethered peptide on surfaces to promote hMSCs differentiation toward osteoblastic lineage. ACS Appl Biomater. 2018;

33. Knippenberg M, Helder MN, Zandieh Doulabi B, Wuisman PIJM, Klein-Nulend J. Osteogenesis versus chondrogenesis by BMP-2 and BMP-7 in adipose stem cells. Biochem Biophys Res Commun. 2006;342(3):902–8.

34. Hoshino M, Egi T, Terai H, Namikawa T, Kato M, Hashimoto Y, et al. Repair of long intercalated rib defects in dogs using recombinant human bone morphogenetic protein-2 delivered by a synthetic polymer and beta-tricalcium phosphate. J Biomed Mater Res - Part A. 2009;90(2):514–21.

35. Gautschi OP, Frey SP, Zellweger R. Bone morphogenetic proteins in clinical applications. Vol. 77, ANZ Journal of Surgery. 2007. p. 626–31.

36. Khan SN, Lane JM. The use of recombinant human bone morphogenetic protein-2 (rhBMP-2) in orthopaedic applications. Expert Opin Biol Ther [Internet]. Taylor & Francis; 2004 May 3 [cited 2018 Sep 25];4(5):741–8. Available from: http://www.tandfonline.com/doi/full/10.1517/14712598.4.5.741

37. Li RH, Wozney JM. Delivering on the promise of bone morphogenetic proteins. Vol. 19, Trends in Biotechnology. 2001. p. 255–65.

38. Javed A, Bae JS, Afza F, Gutierrez S, Pratap J, Zaidi SK, et al. Structural coupling of Smad and RUNX~~unx~~2 for execution of the BMP2 osteogenic signal. J Biol Chem. 2008;283(13):8412–22.

39. Blyth K, Cameron ER, Neil JC. The RUNX genes: Gain or loss of function in cancer. Vol. 5, Nature Reviews Cancer. 2005. p. 376–87.

40. Mercado AE, Yang X, He X, Jabbari E. Effect of grafting BMP2-derived peptide to nanoparticles on osteogenic and vasculogenic expression of stromal cells. J Tissue Eng Regen Med. 2014;8(1):15–28.

41. Chen Z xin, Chang M, Peng Y li, Zhao L, Zhan Y rui, Wang L jing, et al. Osteogenic growth peptide C-terminal pentapeptide [OGP(10-14)] acts on rat bone marrow mesenchymal stem cells to promote differentiation to osteoblasts and to inhibit differentiation to adipocytes. Regul Pept. 2007;142(1–2):16–23.

42. Bab I, Chorev M. Osteogenic growth peptide: From concept to drug design. Biopolym - Pept Sci Sect. 2002;66(1):33–48.

43. McBeath R, Pirone DM, Nelson CM, Bhadriraju K, Chen CS. Cell Shape, Cytoskeletal Tension, and RhoA Regulate Stem Cell Lineage Commitment. Dev Cell [Internet]. 2004 Apr [cited 2014 Oct 19];6(4):483–95. Available from: http://www.sciencedirect.com/science/article/pii/S1534580704000759

44. Kilian KA, Mrksich M. Directing stem cell fate by controlling the affinity and density of ligand-receptor interactions at the biomaterials interface. Angew Chemie - Int Ed. 2012;51(20):4891–5.

45. Meinhart JG, Schense JC, Schima H, Gorlitzer M, Hubbell JA, Deutsch M, et al. Enhanced Endothelial Cell Retention on Shear-Stressed Synthetic Vascular Grafts Precoated with RGD-Cross-Linked Fibrin. Tissue Eng. 2005;11(5/6):887–95.

46. Huang W. Signaling and transcriptional regulation in osteoblast commitment and differentiation. Front Biosci. 2007;12(3068).

47. Kilian K a., Bugarija B, Lahn BT, Mrksich M. Geometric cues for directing the differentiation of mesenchymal stem cells. Proc Natl Acad Sci [Internet]. 2010;107(11):4872–7. Available from: http://www.pnas.org/cgi/doi/10.1073/pnas.0903269107

FIGURE CAPTIONS

Figure 1. Scheme of the different shapes and sizes of patterns

Figure 2. Scheme of preparation of the pattern surfaces

Figure 3. Profilometry images of resist micropatterned surfaces showing three different pattern geometries (hexagons, rectangles, squares).

Figure 4. Fluorescence images of the different patterned surfaces with RGD-TAMRA (labelled in red) and OGP-FITC (labelled in green). Scale bar: 100 µm.

Figure 5. Fluorescent intensity profile of the squared geometry with RGD-TAMRA (labelled in red) and OGP-FITC (labelled in green). Scale bar: 100 µm.

Figure 6. Gene expression dynamics after 2 weeks of RUNX~~unx-~~2, (A: RGD+BMP; D: RGD+OGP), ColI-α1 (B: RGD+BMP; E: RGD+OGP) and osteocalcin (OCN) (C: RGD+BMP; F: RGD+OGP) on different size of patterns (n=5).

Figure 7. Gene expression dynamics after 2 weeks of RUNX~~unx-~~2, (A: RGD+BMP; D: RGD+OGP), ColI-α1 (B: RGD+BMP; E: RGD+OGP) and osteocalcin (OCN) (C: RGD+BMP; F: RGD+OGP) on different shapes of patterns (n=5).

TABLES

Table 1. Nucleotide sequences of primers used for quantitative RT-qPCR detection

Gene	Primer Sequence
RUNX~~unx~~2	5’-AAGTGCGGTGCAAACTTTCT-3’ (Forward)
	5’-TCTCGGTGGCTGGTAGTGA-3’ (Reverse)
Alkaline Phosphatase	5'-ATGCCCTGGAGCTTCAGAAG-3' (Forward)
	5'-TGGTGGAGCTGACCCTTGAG-3' (Reverse)
Osteocalcin	5'-GACTGTGACGAGTTGGCTGA-3' (Forward)
	5'-CTGGAGAGGAGCAGAACTGG-3' (Reverse)
Collagen I α1	5'-ACATGTTCAGCTTTGTGGACC-3' (Forward)
	5'-TGATTGGTGGGATGTCTTCGT-3' (reverse)
PPIA	5'-CGGGTCCTGGCATCTTGT-3' (Reverse)
	5'-CAGTCTTGGCAGTGCAGATGA-3' (Reverse)
RPC53	5'-ACCCTGGCTGACCTGACAGA-3' (Forward)
	5'-AGGAGTTGCACCCTTCCAGA-3' (Reverse)

Table 2. Expected and measured size of the pattern features for the five different geometries.

	Expected size (µm)			Measured size (µm)		
	Length	Width	Gap	Length	Width	Gap
Hexagons	88	76.2	19	81 ± 1	73.6 ± 0.5	18.7 ± 0.5
Squares 100x100	100		17	100,2 ± 0,8		17.0 ± 0.7
Squares 50x50	50		15.5	49 ± 1		16.3 ± 0.7

Squares 25x25	25		9	25.2 ± 0.1		8.8 ± 0.1
Rectangles	50	25	12.5	49.8 ± 0.6	24.8 ± 0.5	12.7 ± 0.5

FIGURES

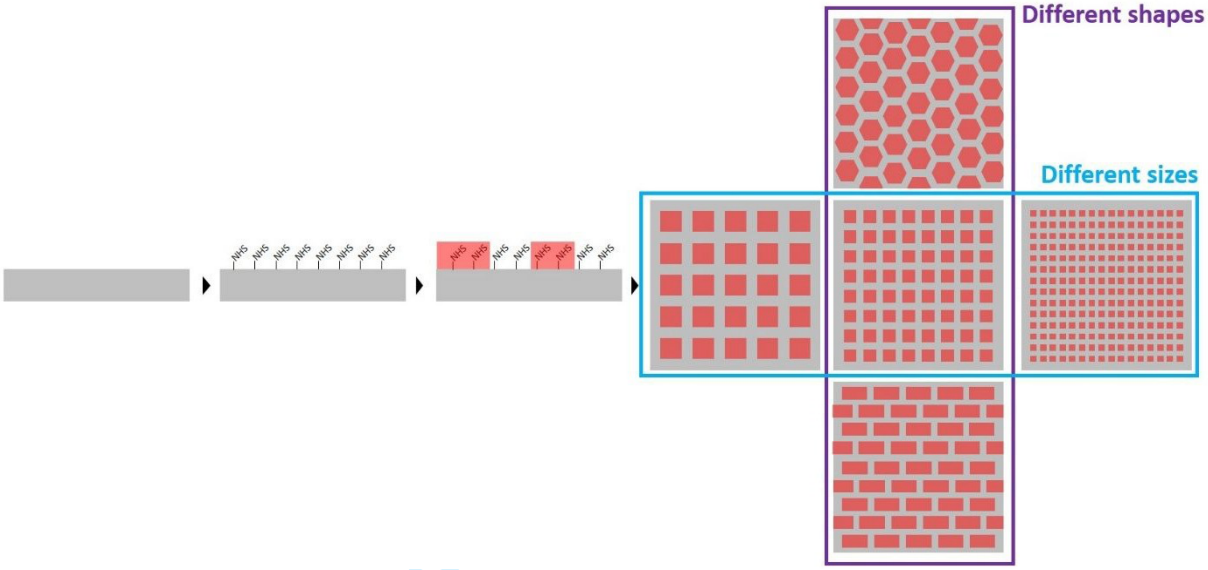

Figure 1. Scheme of the different shapes and sizes of patterns

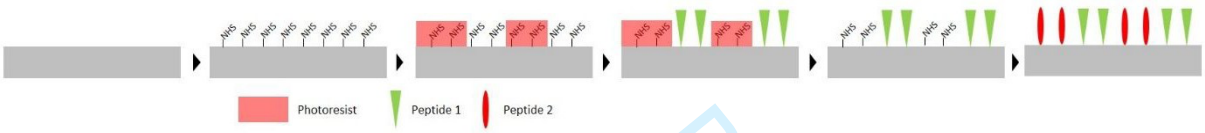

Figure 2. Scheme of preparation of the pattern surfaces

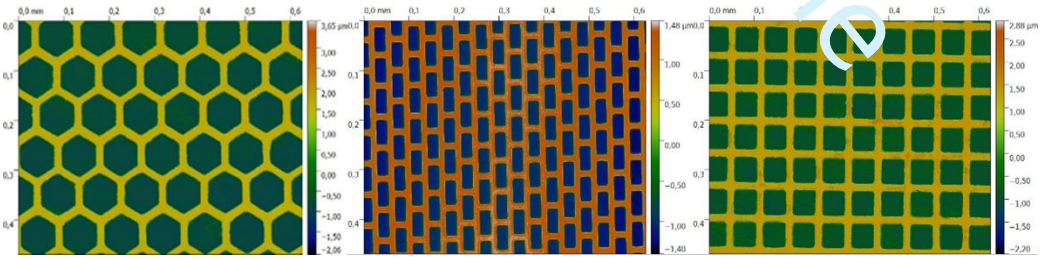

Figure 3. Profilometry images of resist micropatterned surfaces showing three different pattern geometries (hexagons, rectangles, squares).

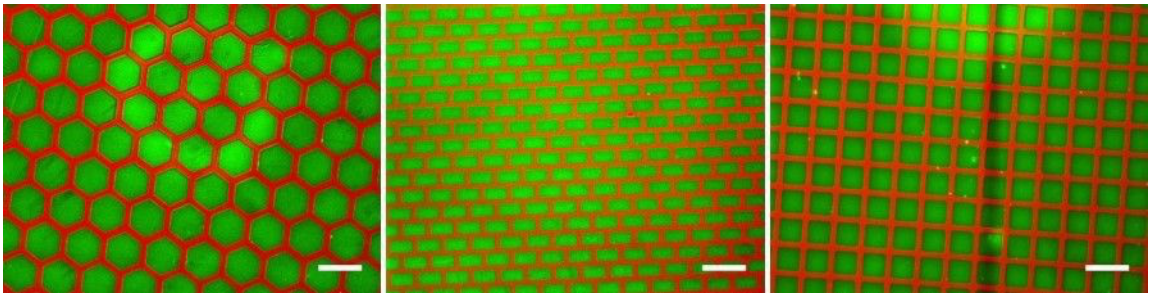

Figure 4. Fluorescence images of the different patterned surfaces with RGD-TAMRA (labelled in red) and OGP-FITC (labelled in green). Scale bar: 100 µm.

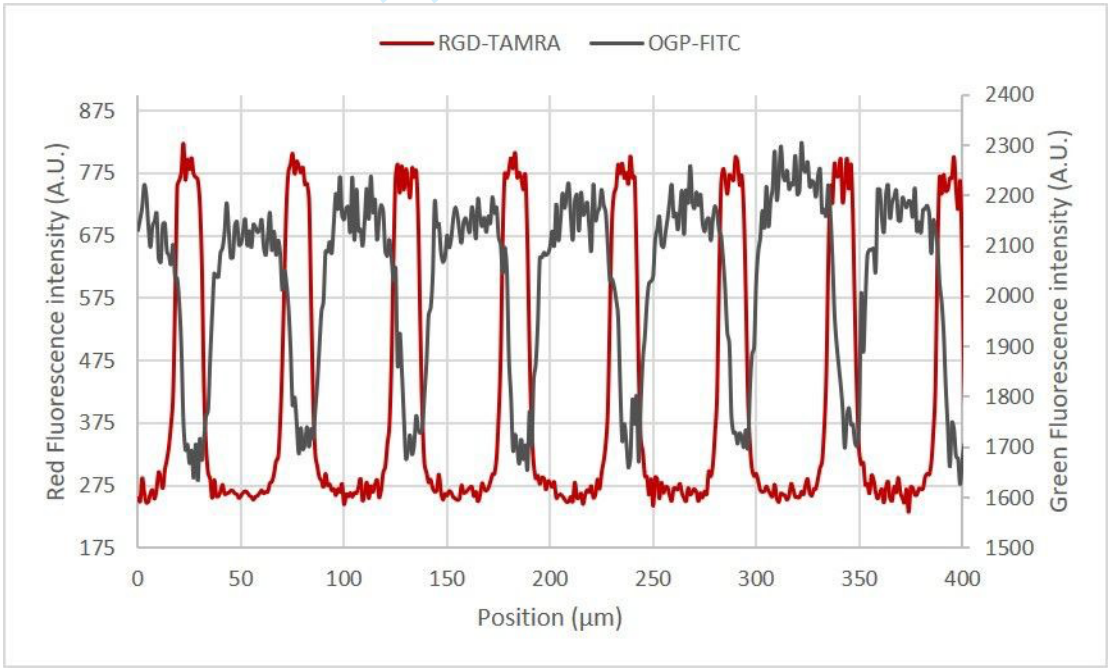

Figure 5. Fluorescent intensity profile of the squared geometry with RGD-TAMRA (labelled in red) and OGP-FITC (labelled in green). Scale bar: 100 µm.

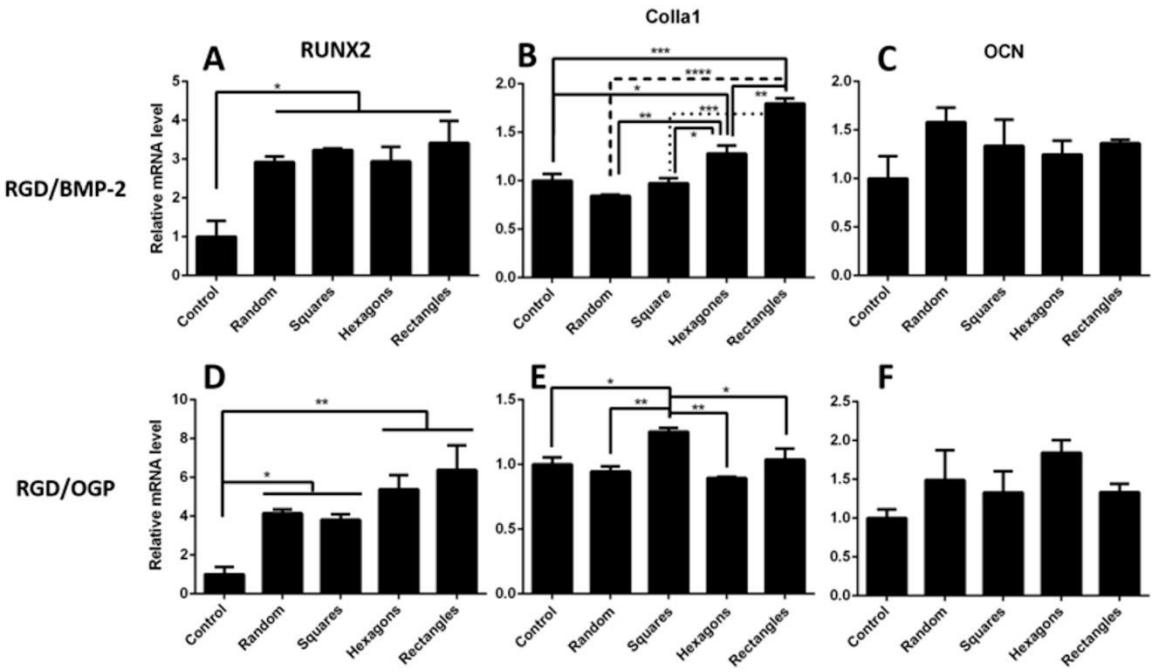

Figure 6. Gene expression dynamics after 2 weeks of ~~Runx-RU~~NX2, (A: RGD+BMP; D: RGD+OGP), ColI-α1 (B: RGD+BMP; E: RGD+OGP) and osteocalcin (OCN) (C: RGD+BMP; F: RGD+OGP) on different size of patterns (n=5).

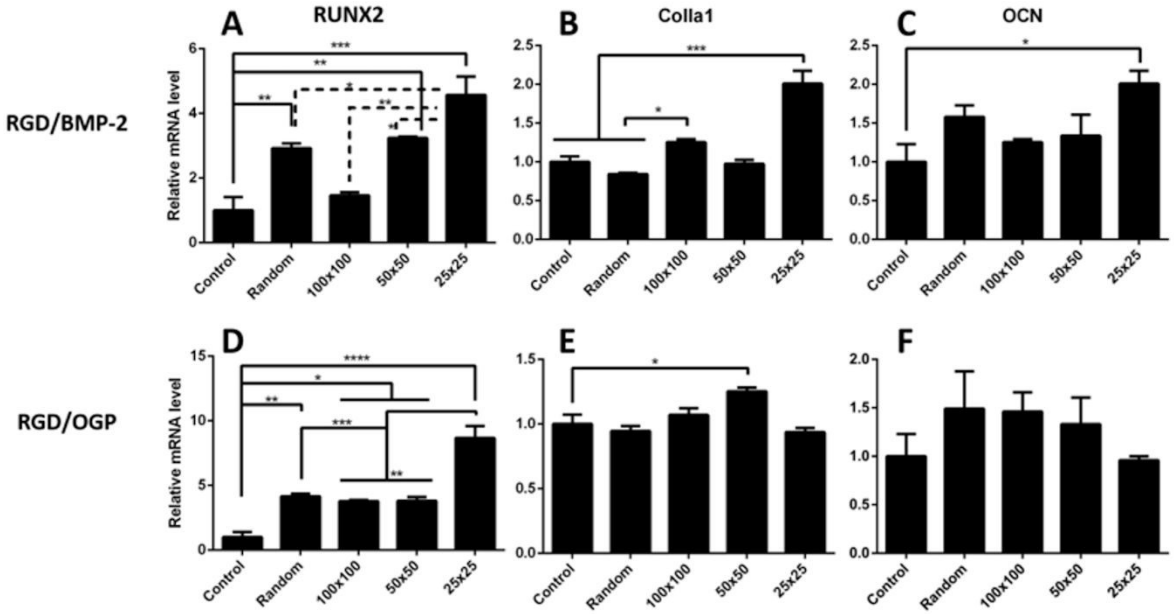

Figure 7. Gene expression dynamics after 2 weeks of ~~Runx-RU~~NX2, (A: RGD+BMP; D: RGD+OGP), ColI-α1 (B: RGD+BMP; E: RGD+OGP) and osteocalcin (OCN) (C: RGD+BMP; F: RGD+OGP) on different shapes of patterns (n=5).

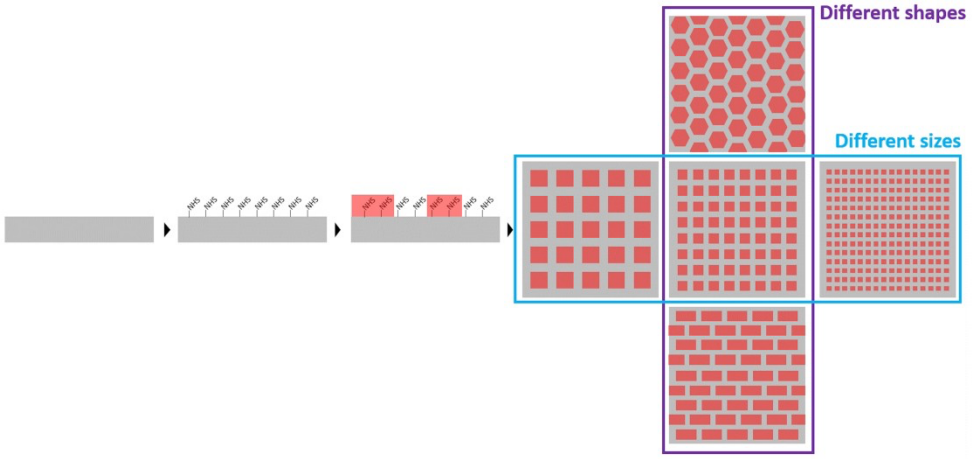

Figure 1. Scheme of the different shapes and sizes of patterns

294x139mm (300 x 300 DPI)

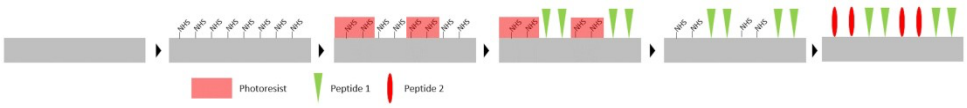

Figure 2. Scheme of preparation of the pattern surfaces

308x34mm (300 x 300 DPI)

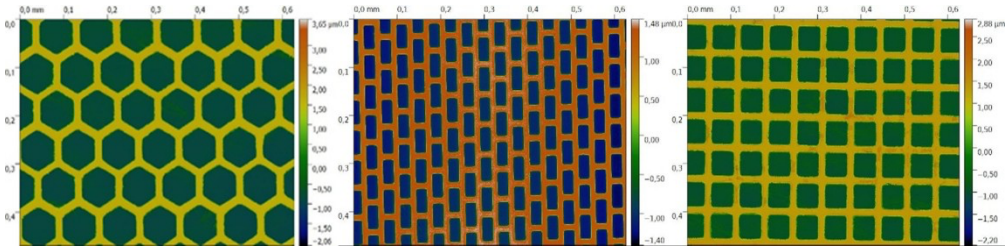

Figure 3. Profilometry images of resist micropatterned surfaces showing three different pattern geometries (hexagons, rectangles, squares).

315x75mm (300 x 300 DPI)

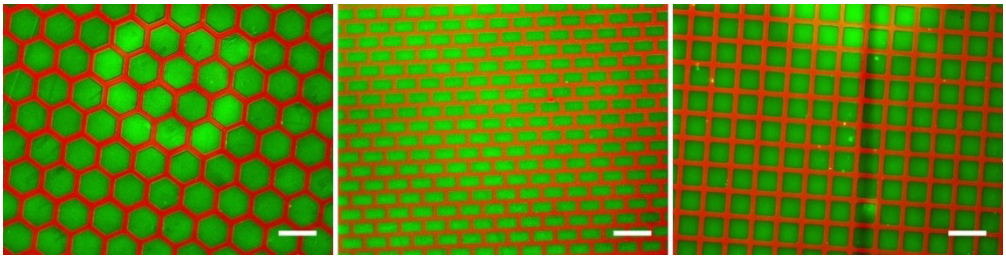

Figure 4. Fluorescence images of the different patterned surfaces with RGD-TAMRA (labelled in red) and OGP-FITC (labelled in green). Scale bar: 100 μm.

393x99mm (300 x 300 DPI)

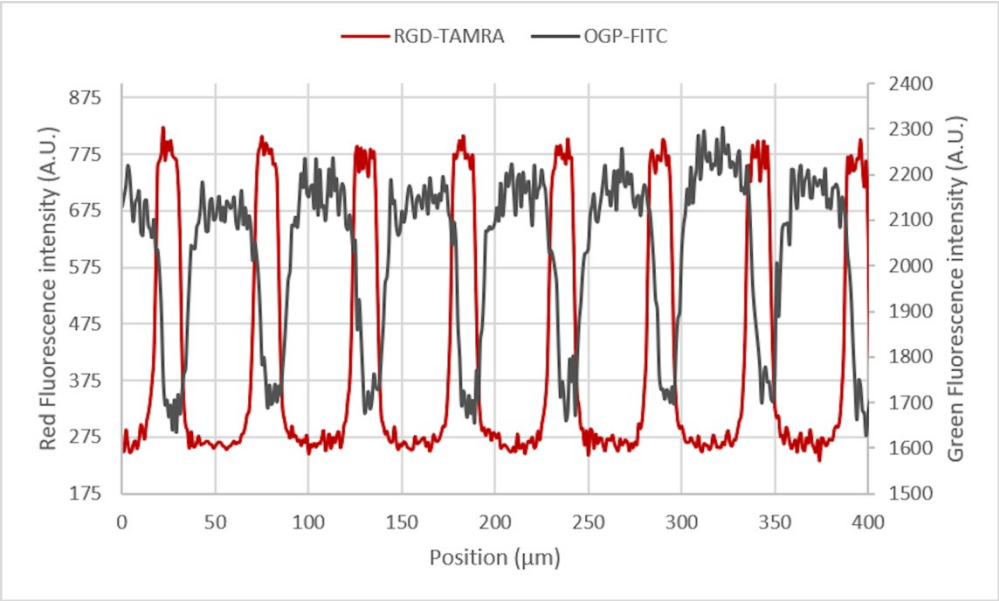

Figure 5. Fluorescent intensity profile of the squared geometry with RGD-TAMRA (labelled in red) and OGP-FITC (labelled in green). Scale bar: 100 µm.

146x87mm (300 x 300 DPI)

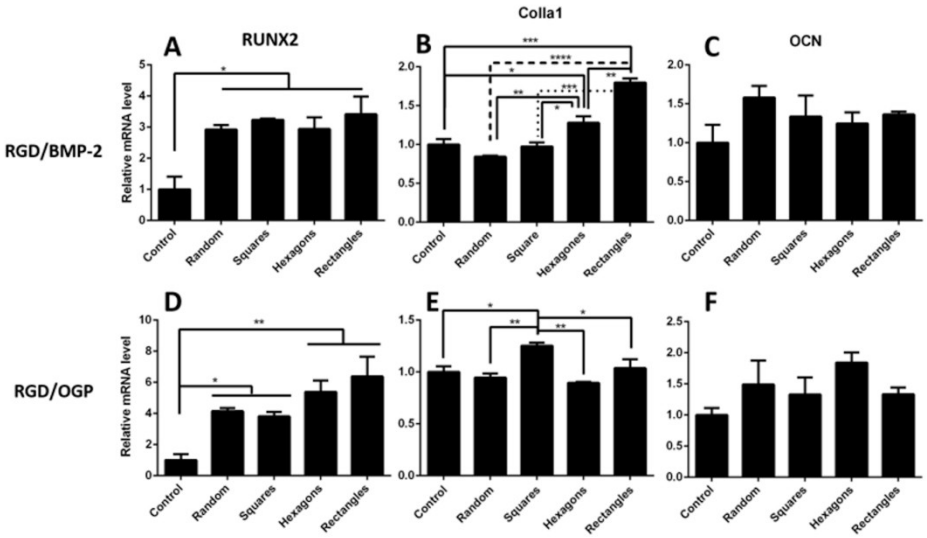

Figure 6. Gene expression dynamics after 2 weeks of RUNX2, (A: RGD+BMP; D: RGD+OGP), ColI-α1 (B: RGD+BMP; E: RGD+OGP) and osteocalcin (OCN) (C: RGD+BMP; F: RGD+OGP) on different size of patterns (n=5).

324x181mm (300 x 300 DPI)

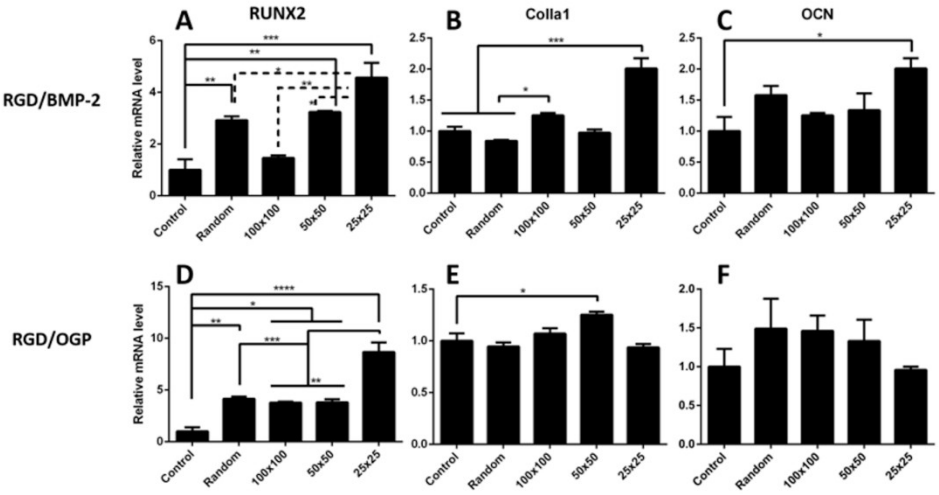

Figure 7. Gene expression dynamics after 2 weeks of RUNX2, (A: RGD+BMP; D: RGD+OGP), ColI-α1 (B: RGD+BMP; E: RGD+OGP) and osteocalcin (OCN) (C: RGD+BMP; F: RGD+OGP) on different shapes of patterns (n=5).

323x174mm (300 x 300 DPI)